Received: 1 October 2024 | Accepted: 21 April 2025 | Published online: 30 April 2025

DOI: 10.53550/ijsc.v53.i1.183

ORIGINAL ARTICLE

Indian Journal of Soil Conservation

Assessing Soil Erosion and Sediment Dynamics in the Balganga Watershed, Uttarakhand: Integration of InVEST-SDR and Fallout Radionuclide (FRN) ^{137}Cs Method

Akanksha Singh[1] | Justin George Kalambukattu[1,*] | Suresh Kumar[2]

[1]Agriculture and Soils Department, Indian Institute of Remote Sensing (IIRS), Indian Space Research Organisation (ISRO), Dehradun, India.

[2]Agriculture, Forestry and Ecology Group, Indian Institute of Remote Sensing (IIRS), Indian Space Research Organisation (ISRO), Dehradun, India.

Corresponding Author:

E-mail: justin@iirs.gov.in; justingeorgek@gmail.com

Handling Editor:

Dr Ashish Pandey

ABSTRACT

Soil erosion assessment in mountainous regions is complex due to rugged topography, dynamic land use, and climate interactions. The revised universal soil loss equation (RUSLE) is widely used for regional soil erosion estimation, but it often overestimates soil loss in such landscapes. This study, conducted in the Balganga watershed of Tehri Garhwal, Uttarakhand, integrates the Integrated Valuation of Ecosystem Services and Tradeoffs-Sediment Delivery Ratio (InVEST-SDR) model to provide a more refined estimation of annual soil erosion, sediment export, and retention. Field-based soil sampling was carried out across 21 physiographic units, followed by targeted laboratory analysis. The InVEST-SDR model was applied in two stages: (1) estimating soil erosion using RUSLE and (2) computing the sediment delivery ratio to determine sediment export and retention. The results indicate that potential annual soil loss in the watershed ranges from 0 to 67.63 t ha^{-1}yr^{-1}, with an average of 16 t ha^{-1}yr^{-1}. The average sediment export was 1.52 t ha^{-1}yr^{-1} (range: 0 to 10.5 t ha^{-1}yr^{-1}), while sediment retention averaged 22.68 t ha^{-1}yr^{-1}, reaching up to 60 t ha^{-1}yr^{-1}. To validate the model, the Fallout Radionuclide (FRN) ^{137}Cs method was employed to estimate observed soil loss across major land use/land cover (LULC) classes. A moderate correlation ($R^2 = 0.51$) was found between observed and modeled soil loss values, with a Mean Absolute Error (MAE) of 3.593, indicating reasonable predictive accuracy. The erosion assessment revealed that 58.11% of the watershed falls under the very low erosion class, while scrublands (35.51 t ha^{-1}yr^{-1}) and agricultural lands (16.68 t ha^{-1}yr^{-1}) on steep slopes exhibited the highest erosion rates. Scrublands also had the highest sediment export (3.52 t ha^{-1}yr^{-1}), followed by agricultural lands (2.29 t ha^{-1}yr^{-1}). Conversely, well-managed valley agricultural lands demonstrated significant sediment retention (25.84 t ha^{-1}yr^{-1}) from upstream sources. The study highlights vegetation cover, conservation practices, and soil erodibility (K-factor) as critical factors influencing erosion patterns. These findings reinforce the importance of integrating empirical and modeling approaches for improved erosion assessment and sustainable watershed management in fragile mountainous regions.

Key words:

Balganga watershed
FRN ^{137}Cs
Himalaya
InVEST-SDR
Physiographic analysis
Sediment export
Soil erosion

1 | INTRODUCTION

Soil erosion is one of the main challenges affecting soil quality among the different issues. The global average soil erosion rate is estimated to range from 12 to 15 t ha^{-1}, which is more than the rate at which soil is formed (Boardman, 2021). According to numerous field-based studies conducted at various locations and river basins, the Himalayas were found to exhibit extremely high rates of soil erosion, ranging from 20-25 t ha^{-1}yr^{-1} to even 92 t ha^{-1}yr^{-1} (Swarnkar *et al.,* 2018). The tolerance limit of 11.2 t ha^{-1}yr^{-1} for soil loss is exceeded in approximately 48.3% of Uttarakhand (Mandal and Sharda, 2011), which highlights the necessity of implementing suitable soil and water conservation measures to reduce topsoil loss in the delicate Himalayan ecosystem A study conducted in the region estimated an average annual soil erosion value of 27.45 t ha^{-1}yr^{-1} (Kalambukattu *et al.,* 2021).

Assessing the annual rate of soil erosion is crucial for identifying high and low-risk areas with respect to susceptibility. A region's susceptibility to soil loss can be determined using a variety of techniques, depending on factors such as topography, soil quality, land use, and more. Field-based measurements like erosion or runoff measurement and sediment sampling in watersheds are highly regarded, but they are impractical for large spatio-temporal scales. Therefore, models are employed to predict outcomes at varying spatial and temporal scales for different land use and land cover conditions. Numerous researchers have employed an extensive range of techniques, such as empirical, semi-empirical, physical, and statistical models, to predict soil erosion. Researchers have widely used various models to predict soil erosion rates at various scales, differing in processes considered, complexity, and data requirements. These include empirical models like the universal soil loss equation (USLE), agricultural nonpoint source model (AGNPS), revised universal soil loss equation (RUSLE), chemical runoff and erosion from agricultural management systems (CREAMS), and modified universal soil loss equation (MUSLE); semi-empirical models like the annualized agricultural non-point source (AnnAGNPS), soil and water assessment tool (SWAT), and hydrologic simulation program fortran (HSPF); and physical models like the limburg soil erosion model (LISEM), water erosion prediction project (WEPP), and european soil erosion model (EUROSEM) (Karydas *et al.,* 2014). Among all these, RUSLE model has been widely recognized and implemented globally for assessing erosion risk at various scales and landscapes (Achu & Thomas, 2023; Ramachandran *et al.,* 2023). This can be attributed to its modest data requirements, robust and easily understandable structure, and compatibility with remote sensing and GIS. These features make it particularly suitable for regions where other complex models are impractical due to high data requirements and costs. Although RUSLE models the long term average annual erosion, it does not account for modeling the transportation or deposition of the eroded soil particles. However while planning conservation measures and strategies in a watershed; knowledge regarding all these aspects of erosion process becomes important, especially in high erosion risk region like the Indian Himalayas. There are a few models capable of modeling sediment transport in a region like Instantaneous Unit Sediment Graph (Williams, 1978), LAS CAM (Viney & Sivapalan, 1999) etc.

Many empirical models fail to incorporate dynamic value changes in spatial domains and the complexities of spatial inputs. Consequently, researchers have utilized the ecosystem services model, InVEST software suite, particularly the sediment delivery ratio (SDR) module. This module effectively maps and estimates soil loss, export, retention, and sediment reaching rivers based on RUSLE. Its application spans various scales and landscapes such as river basins (Bouguerra & Jebari, 2017), hilly-mountainous regions (Wang *et al.,* 2020), watershed (Degife *et al.,* 2021), plateaus (Liu *et al.,* 2023) and mixed landscapes (Guo *et al.,* 2023), demonstrating model versatility. In India, few studies have utilized the InVEST-SDR model (Kantharajan *et al.,* 2023), particularly in the hilly mountainous region of north-western himalaya.

HIGHLIGHTS

- Erosion Modeling Approach - The study integrates InVEST-SDR with RUSLE modeling to enhance soil erosion predictions in mountainous regions.
- Fallout Radionuclide (FRN) ^{137}Cs technique was used to validate modeled soil loss, providing empirical evidence for erosion estimates.
- Scrublands and agricultural areas exhibit the highest soil erosion and sediment export, while valley agricultural lands effectively retain sediment due to good management practices.

Assessing models' capabilities across regions and scenarios is essential, as they only approximate natural processes. Validation typically involves field surveys to gather observed values of erosion, sediment export, and retention from experimental plots. However, traditional methods are better suited for flat lands than for the highly undulating mountainous regions, where experimental plots are prone to washout from extreme runoff events, leading to inaccurate measurements. In rugged terrains, various factors influence erosion processes at different rates, causing rapid changes over short distances. To address these challenges, the Fallout RadioNuclide (FRN) ^{137}Cs method is increasingly used for validation. The use of radioactive Caesium dates back to the 1960s, when studies on Caesium-137 dynamics with soil emerged (Rogowski and Tamura, 1965). The Cs technique reliably quantifies net soil erosion, serving as a validation strategy for spatial soil erosion rates estimated by the SDR module. Integrating the InVEST model with the Cs method could provide a comprehensive assessment of soil erosion dynamics and sediment transport pathways, aiding watershed management and sediment control strategies. However, no attempts have been reported in the Northwestern Himalayan region to model soil erosion risk and sediment export at a watershed scale. This study aims to quantify the spatial variability of soil erosion and sediment delivery / retention rates in a hilly watershed using the InVEST model and validate it with the Cs technique. The study is expected to advance geospatial techniques in understanding soil erosion processes, supporting informed decision-making for sustainable land use planning and environmental conservation.

2 | MATERIALS AND METHODS

2.1 | Study Area

The study was conducted in the Balganga watershed, a part of Tehri dam catchment, located in the Tehri Garhwal district of Uttarakhand India (*Fig.1*). It is one of the four major sub catchments of the Tehri dam located on the Bhagirathi River. Balganga River is a significant tributary of the Bhilangana River, which confluences with the latter at Ghansali, located 3 km downstream of Sarasgaon, at an elevation of 818 m, before discharging directly into the reservoir. The watershed lies between 30.15° N and 30.42° N latitudes and 78.23° E and 78.63° E longitudes, covering an area of 48,800 hectares. This region blends in the lesser, middle, and the greater Himalayan ranges, forming a magnificent and diverse landscape progressing upwards, with an elevation ranging from 793 m to 4785 m. The region features high mountain ranges, broad valleys, deep gorges and spurs. Balganga range, which occupies the upper stretches of the study area, is covered by dense evergreen forest. The climate of the area varies considerably with elevation, being cold temperate in the higher reaches and subtropical at lower elevations. Even though the area receives year-round rainfall, the summer monsoon season brings the highest percentage of rainfall (83%) to the area. Forests, grasslands, scrublands, barren areas and croplands form the major land use land cover (LULC) types in the area. Subsistence farming is practiced in most parts of the area, with a wide variety of crops such as paddy, maize, wheat, barley, pulses, vegetables etc cultivated in different seasons. The forest cover can be classified as either dense forest or open forest based on the tree canopy cover. Oaks (*Quercus leucotrichophora*), Deodar (*Cedrus deodara*), Pine (*Pinus roxburghii*), and Buransh (*Rhododendron arboreum*) represent the predominant forest species observed in the watershed.

2.2 | Data Used

Various remote sensing data derived thematic and auxillary data were used in this study for spatial modelling. The ALOS PALSAR digital elevation model (DEM) Level 2.2

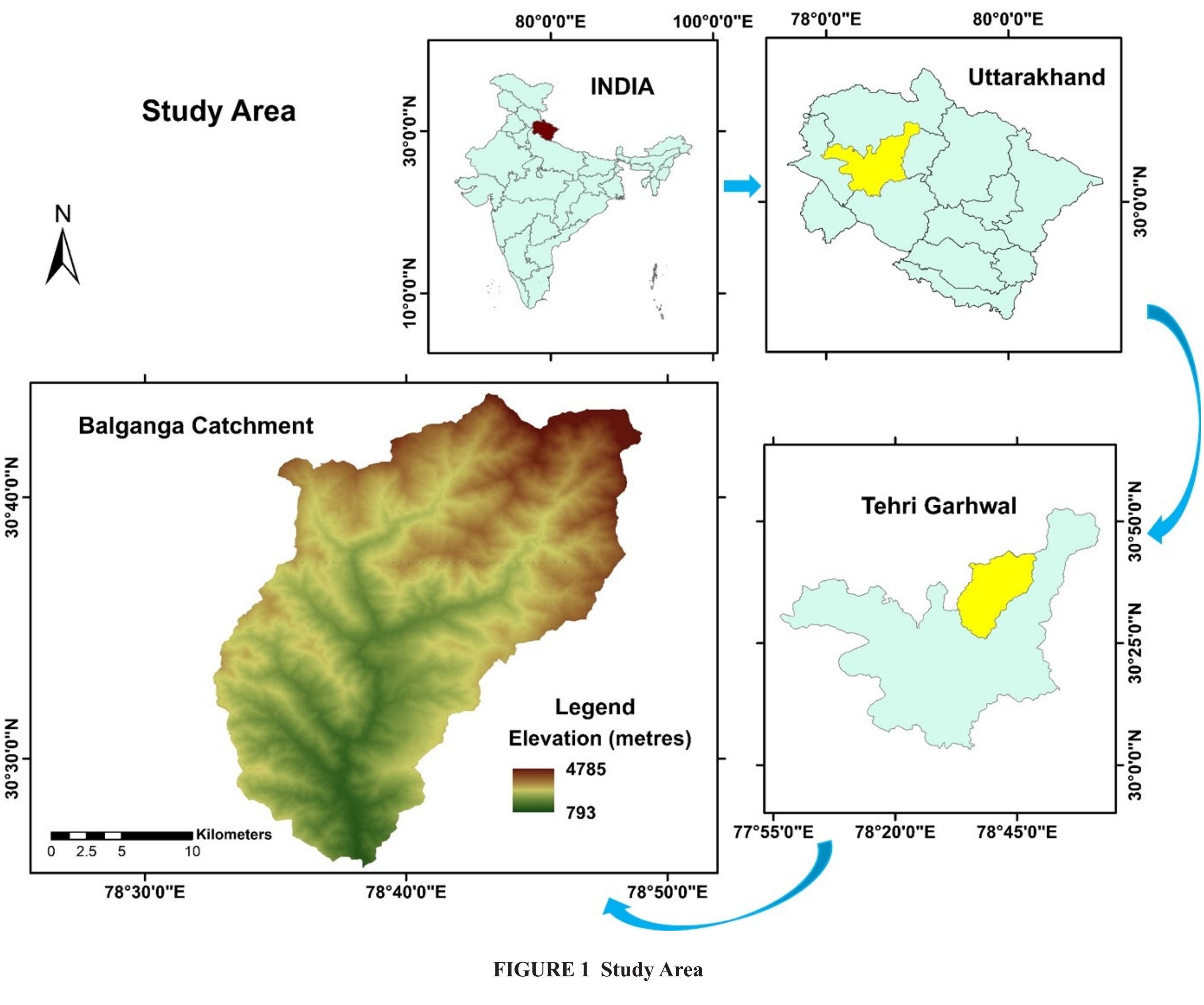

FIGURE 1 Study Area

image of 12.5m spatial resolution was downloaded from https://asf.alaska.edu/datasets/daac/alos-palsar/ and processed using ArcGIS 10.3 for producing various topographic parameters using digital terrain analysis. These terrain parameters were further used in erosion modelling as well as spatial prediction of erodibility factor. For identifying and classifying the current land use land cover map (LULC), Sentinel 2 dataset (10m resolution) was classified using random forest algorithm in google earth engine (GEE) platform. LULC map based on advanced wide field sensor (AWIFS) data from Bhuvan (https://bhuvan.nrsc.gov.in) was also used for modification and preparation of final LULC map of the study area. Similarly for generation of temporal normalized difference vegetation index (NDVI), enhanced vegetation Index (EVI) and LULC maps, Landsat time series RS data (30 m resolution) were accessed using Google Earth Engine starting from 1980 till date at every 20 years' interval. Thus, the temporal RS data from Landsat series (Landsat 3 to Landsat 9) were used for the generation of temporal C- factor maps, representing the long-term vegetation cover. For the estimation of long-term rainfall erosivity values and generating spatial distribution maps of Rainfall erosivity factor in the area, the average yearly rainfall erosivity was calculated for the time period starting from 1963 to 2022 (59 years), using IMD gridded (0.25° * 0.25°) dataset which can be downloaded from https://imdpune.gov.in/cmpg/Griddata/Rainfall_25_Bin.html (Pai *et al.,* 2014). The downloaded data were then compiled for all years using microsoft excel soil samples collected during field survey were analyzed in the laboratory for estimation of different soil properties and computation of soil erodibility factor values (K factor).

2.3 | Field data collection and soil analysis

A stratified random sampling approach based on dominant soil-landscape units was adopted for the collection of soil samples from the study area. The soil-landscape unit map of the area was generated by combining the topographic position index (TPI) based landform element map, aspect map and LULC map of the area. This sampling strategy can provide an accurate representation of variability in the entire region except for the uppermost parts of the watershed, which are inaccessible. Surface and subsurface soil samples were collected from 120 georeferenced locations covering 21 different strata/physiographic units, during the field survey conducted in December 2023. These physiographic units represent unique combinations of hillslope elements, slope aspect, and land use land cover types present in the area and determining the variability of soil properties. The procedure followed in the generation of these sampled strata (Table 2) is detailed in the later sections. During sampling, utmost care was given to avoid sampling from locations adjacent to roads, waterbodies, as well as recently manured and irrigated fields. The collected samples were packed, securely transported and preprocessed for laboratory analysis. The preprocessed and sieved samples were analyzed in the laboratory for estimation of different properties namely pH using pH meter, electrical conductivity using an (EC) meter, soil organic carbon (SOC) using walkley and black titration method (WBTM) and textural composition using Bouyoucos Hydrometer method, employing standard analytical procedures. The soil database thus generated was used for the computation of soil erodibility values at different sampling location.

2.4 | Overall Methodology Adopted

The study employed InVEST model estimation and mapping of soil erosion, export and retention and validated the results using FRN ^{137}Cs method. The InVEST Model is a robust and self-contained suite of Ecosystem Services assessment models developed by the Natural Capital Project, a collaboration of various academic institutions and conservation non-governmental organizations in 2009 for assessing ecosystem services and land use changes. It requires minimal input data due to the incorporation of simplified hydrological processes within the model architecture. It offers a distinct advantage over RUSLE by overcoming it's constraints and thus enabling the holistic assessment of soil loss, sediment export, and sediment retention at varying scales. This is achieved through the characterization of hydrological connectivity within a specific watershed (Sharp *et al.,* 2018). It quantifies and maps soil erosion within watersheds, automatically using the spatial resolution of input DEMs. The sediment delivery ratio (SDR) module evaluates sediment export and retention by quantifying annual soil loss (RUSLE) and calculating the fraction of it reaching streams, assuming it ends at the catchment outlet, without considering in-stream processes. The overall methodology adopted in the study is depicted in *Fig. 2*.

2.4.1 | Model Workflow

The sediment delivery ratio (SDR) module developed by InVEST was used for the computation and spatial mapping of overland sediment flow, amount of sediment delivery to the stream, and amount of sediment retention by topographic and vegetative features on an annual basis. *Fig. 3* illustrates the various input parameters required in different formats by the model for computation of erosion, sediment export as well as retention. The primary goal of SDR module is to model how landscape management affects the generation, delivery, and retention of sediment in watershed and how the results could be used for watershed management. The model employs the revised universal soil loss equation (RUSLE) to quantify the pixel-by-pixel annual soil loss and further it calculates the sediment delivery ratio, or the percentage of soil loss that actually reaches the

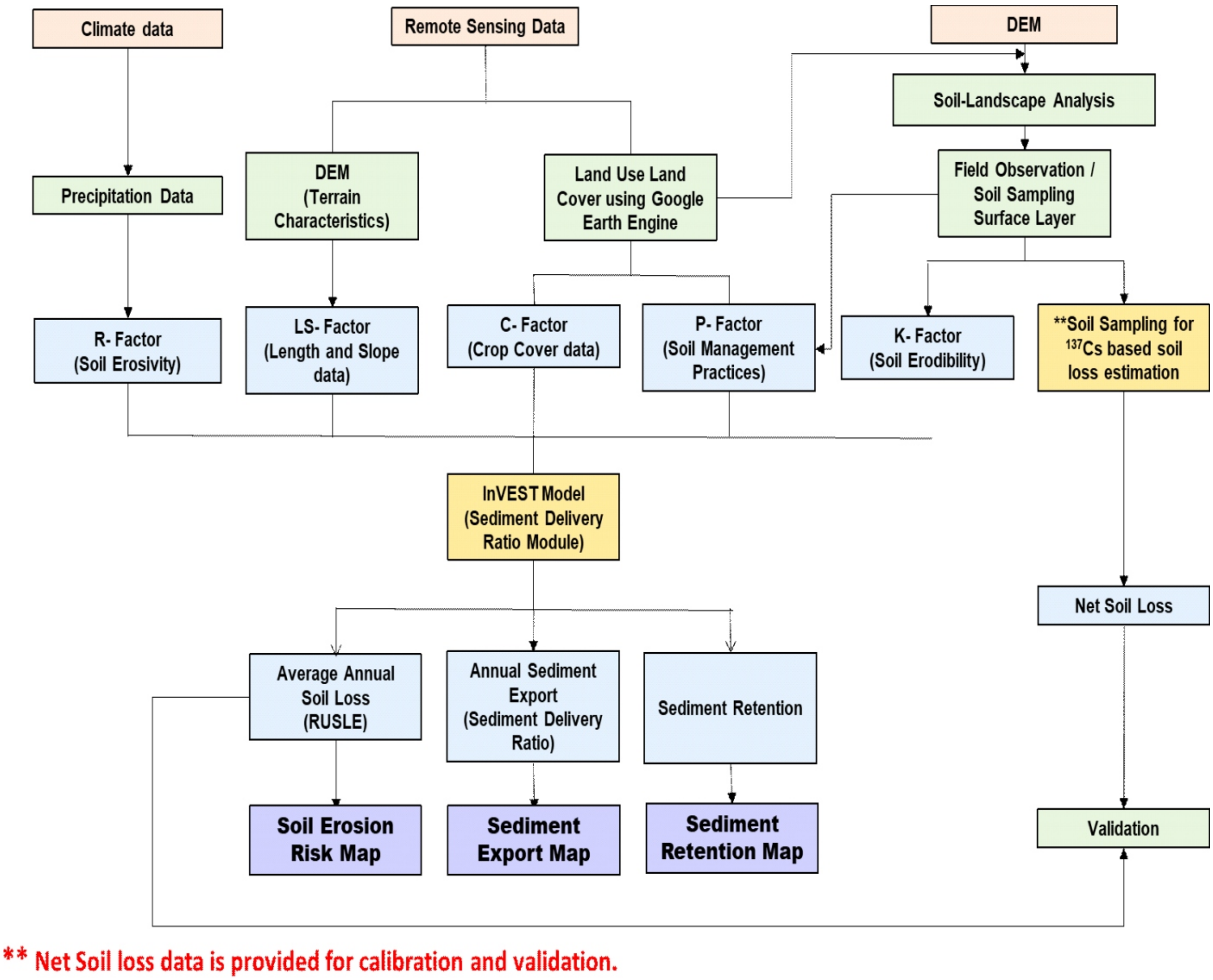

FIGURE 2 **Overall Methodology adopted in the study for modeling Soil Erosion, Export and Retention using InVEST Model**

stream. The different steps involved along with the generation and utility of various input parameters in the model are discussed in the following sections.

Step 1: Estimating the Annual Soil Loss

The revised universal soil loss (RUSLE) equation is used by the SDR model from the InVEST suite to estimate the annual soil loss (A, measured in tons per hectare per year, t ha^{-1} yr^{-1}) on each pixel. Mathematically, the model could be expressed as:

$$A = R * K * LS * C * P$$

Where A - long-term average annual soil loss (t ha^{-1}yr^{-1}), R - rainfall erosivity factor (MJ mm ha^{-1}h^{-1}yr^{-1}), K - soil erodibility factor (t ha h ha^{-1}MJ^{-1}mm^{-1}), LS - slope length - steepness factor, C - crop cover factor and P - conservation practice factor.

- **Rainfall Erosivity factor ®**: This factor computes the amount and rate of runoff that is directly related to different rainfall events and measures the impact of precipitation as kinetic energy for causing erosion processes. Nine IMD grid stations located around the study area were selected and IMD's (0.25° × 0.25°) gridded rainfall data from 1963-2023 was accessed and processed using Google Colab notebook for estimation of monthly as well as annual rainfall. The R factor was computed using the following equation given by Chen *et al.*, 2023:

$$R = 17.02 * 10^{\left(1.50 * \log \Sigma_1^{12} \frac{pi^2}{p} - 0.8188\right)}$$

Where, *Pi* stands for monthly rainfall (mm), *P* for annual rainfall (mm), and *R* is a rainfall erosivity factor (MJ mm ha^{-1}h^{-1}yr^{-1}).

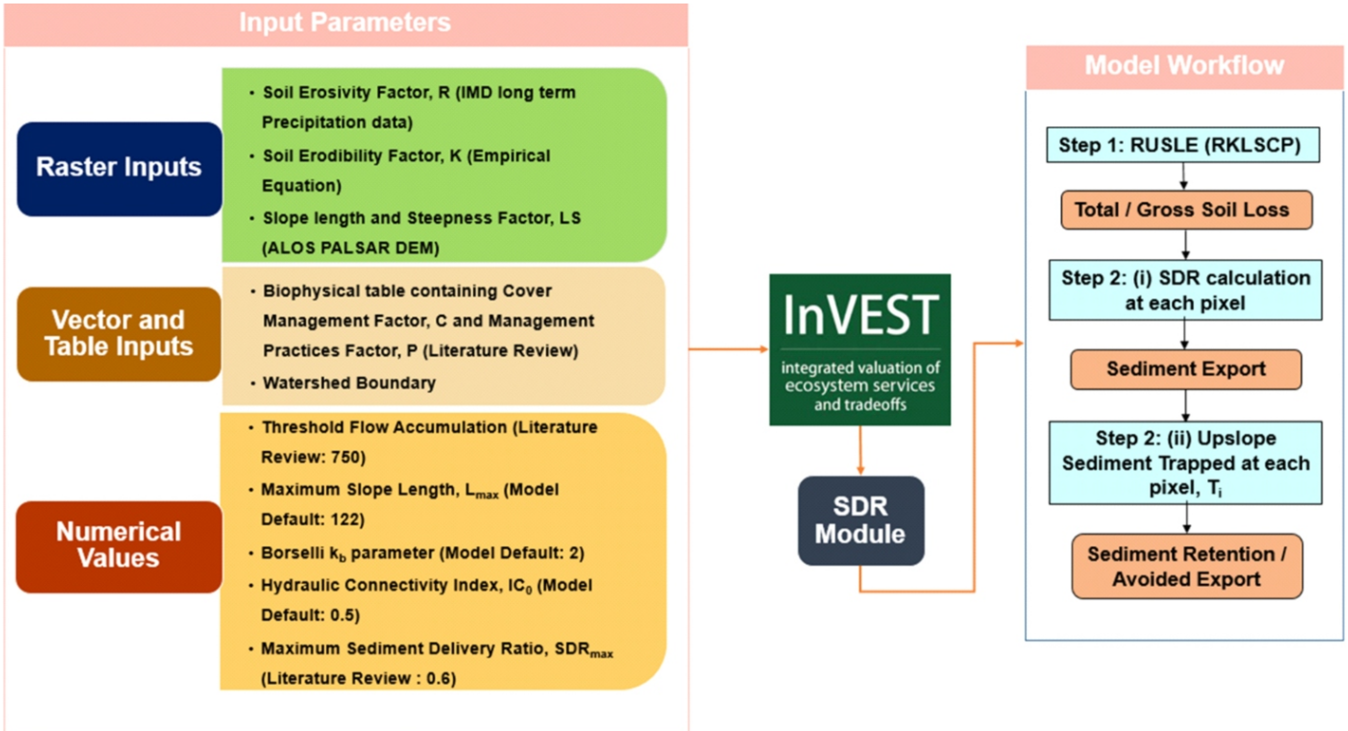

FIGURE 3 Different inputs parameters and model workflow for computation of erosion, sediment export and retention using SDR module of InVEST model

R factor values computed for each station were then interpolated using geostatistical analyst tool in ArcGIS 10.5, to generate the spatial distribution map of rainfall erosivity covering the entire watershed.

- **Soil Erodibility factor, (K)**: It measures the rate at which raindrops can disperse and separate the soil particles and indicates the ability of a soil to resist or permit erosion. The K values were calculated for each sampling location using the analytical data pertaining to SOC content and textural composition, using the following equation given by Sharpley *et al.* (1993).

$$K = 0.1317 * \left(0.2 + 0.3 * e^{\left[-0.0256*SAN\left(1-\frac{SIL}{100}\right)\right]} * \left(\frac{SIL}{CLA+SIL}\right)^{0.3}\right) * \left[1 - \frac{0.25 * TOC}{TOC + e^{(3.72-2.95*TOC)}}\right] * \left[1 - \frac{0.7 * SN_1}{SN_1 + e^{(22.9*SN_1-5.51)}}\right]$$

Where, K is soil erodibility factor (t ha h ha-1 MJ-1 mm-1), SAN is sand weight content (%), SIL is silt weight content (%), CLA is clay weight content (%), TOC is soil organic carbon content (%), SN1=1 – (SAN / 100).

K factor values computed for all the sampling location were used for mapping the spatial distribution of erodibility in the entire study area, using a digital soil mapping approach. Random forest regression (RF) based machine learning technique integrating climatic, vegetative and topographic parameters with erodibility values at sampling location was used for the spatial mapping of erodibility in the entire area. The different environmental covariates used for mapping K factor included rainfall erosivity (R), vegetation parameters including normalized difference vegetation index (NDVI), enhanced vegetation index (EVI), cover management factor (C), support practices factor (P), LULC and topographic parameters namely elevation, slope, aspect, terrain wetness index (TWI), topographic position index (TPI), stream power index (SPI), plan curvature, profile curvature, slope length and steepness factor (LS). All the variables were integrated and used for calibrating the RF model for soil erodibility prediction. The validated model was used for generating spatial distribution maps of soil erodibility in the area.

- **Slope length - slope steepness factor (LS factor):** It accounts for the impact of topography in determining soil erosion processes and rates. The major topographical features that potentially influence runoff and erosion are slope length (L) and steepness (S). The LS factor was computed using ALOS PALSAR DEM (12.5m) employing the equation given below, which is based on the unit-contributing area concept of Desmet & Govers, 1996.

$$L_{ij} = \frac{\left(A_{i,j-in} + D^2\right)^{m+1} - A_{i,j-in}^{m+1}}{D^{m+2} * x_{i,j}^{m} * 22.13^{m}}$$

Where, $A_{i,j-in}$ denotes the contributing area at the inlet of grid cell (*i,j*) measured in m^2. D indicates the grid cell size in meters, , $x_{i,j}^{m} = sin\ sin\ a_{i,j} + cos\ cos\ a_{i,j}$, the $a_{i,j}$ is the aspect direction of the grid cell (i,j) and m represents the standard slope length exponent (ranges from 0 to 1 and indicates the ratio of rill to inter rill erosion) and L_{ij} indicates equivalent slope length factor for the cell.

- **Cover management factor (c):** It represents the combined influence of crops and vegetative cover on reducing soil erosion by protecting soil surface from the direct impact of rainfall. A hybrid methodology involving the use of literature values for agricultural areas while using remote sensing (Landsat) derived NDVI based C factor values for forested areas was adopted in the study. GEE platform was used for accessing temporal RS images for the years 1980, 1992, 2009, 2015, and 2022, to analyze the dynamic nature of vegetation and its temporal variability. For all the chosen years, satellite images of preceding five years/decade were selected, and processed for the generation of average NDVI image for the corresponding year. The equation given below proposed by Durigon *et al.* (2014) was used for the computation of C factor using NDVI images.

$$C = (-NDVI + 1)/2$$

- **Support Practice factor, (P):** It is also referred as conservation practice factor and indicates the role of various conservation and management practices in controlling erosion. Various conservation practices like terracing, contour farming, and strip farming are known to reduce erosion and thus have lower P factor values, whereas higher values towards one indicates no or very less conservation practices and higher erosion potential. In the current study, different LULC classes identified in the area were assigned literature based P factor values according to the management strategies used in these classes.

Step 2: Estimation of Sediment Export and Retention

Sediment delivery ratio (SDR) is the ratio of amount of sediment yield from a region to the total amount of soil eroded from the same region. The major factors affecting the SDR from a location are the land use/ land cover type, soil type (prominently texture and structure), slope characteristics and anthropogenic intervention in the region.

In the model, the value of SDR is obtained in two stages. First, the model computes the pixel-wise connectivity index (IC) which represents the hydrological connectivity relationships between the sediment sources (upstream landscape) and sediment sinks (e.g. streams). It is a function of upslope area (Dup) and the downstream flow path between the pixel of interest and the nearest stream (Ddn). Higher values of this index correspond to greater sediment export and vice versa. It is calculated as per the relationship given by Borselli *et al.* (2008). Second step is to derive the SDR from a pixel based on the ratio of the maximum SDR (SDR_{max}) which is the theoretically possible maximum SDR value for the area, connectivity index, and the calibration parameter as suggested by Borselli *et al.* (2008).

- **Sediment Export:** Sediment export refers to the quantity of the sediment which actually gets exported from a pixel and reaches the stream. This is calculated by multiplying the sediment delivery ratio from a pixel, SDR_i by the total soil erosion from that particular pixel, A_i. The total sediment export, SE, from every pixel in the catchment is then computed by simply summing up all the individual export values, SE_i, from every pixel. It is calculated as:

$$SE_i = A_i * SDR_i \longrightarrow SE = \sum_i SE_i$$

- **Sediment Retention:** In the model, this term is represented as *Avoided Export* by default, which is used to describe an ecosystem service recognized by the downstream users of a watershed. The sediment retention or avoided export value from each pixel indicates the cumulative amount of sediment trapped within a pixel. This parameter exhibits the function of vegetation and management practices (if present) in a region in trapping the upstream sediments and thus restricting them from going downstream into the waterways. It is calculated as:

$$AEX_i = (RKLS_i - USLE_i) * SDR_i + T_i$$

Where, AEX_i is the total sediment retention provided by that pixel, including both on-pixel and upslope erosion sources in tons/pixel/year (t $pixel^{-1}yr^{-1}$); $RKLS_i$ is the total potential soil loss per pixel in the land cover without considering C and P factors or soil loss equivalent from bare soil in (t $pixel^{-1}yr^{-1}$); $USLE_i$ (A_i) is the total potential soil loss per pixel in the land cover considering the effects or cover management factor, C and support practices factor, P in (t $pixel^{-1}yr^{-1}$); SDR_i is the sediment delivery ratio from the pixel and T_i is the amount of upslope sediment that is trapped on that pixel keeping it from entering the stream (t $pixel^{-1}$ yr^{-1}).

Spatial Distribution of Soil Erosion, Export and Retention

The SDR module of the InVEST software suite maps and estimates the potential annual average soil loss, sediment export and sediment retention of the watershed; hence, it should not be confused with the actual values. The spatial outputs are generated in tif format and ArcGIS software was used for input data preparation, result interpretation and further analysis.

2.4.2 | Model Validation

The ^{137}Cs inventory in various landscape units within the study area was obtained from Agriculture and Soils

Department, IIRS. Soil samples for ^{137}Cs analysis were collected using a stratified random sampling technique. Soil samples from a total of 15 sites belonging to different soil landscape units were collected, pre-processed and analysed for ^{137}Cs activity. ^{137}Cs activity in the samples were measured using gamma spectroscopy method (GSM) at the centre for advanced research in environmental radioactivity (CARER), Mangalore, Karnataka. More detailed description of the site selection, sampling procedure, sample pre-processing and radioactivity measurement could be accessed in Kumar *et al.* (2024). The measured radioactivity inventory from samples were then used for the computation of net soil erosion values utilizing different conversion models, which are the Simplified Mass Balance Model / Mass Balance Model I for cultivated agricultural lands, and the Profile Distribution Model for the uncultivated forest regions. The model's projected soil erosion values were validated with the computed net soil erosion values derived from the ^{137}Cs inventory at the sampling sites. The mean soil loss for each site (7*7-pixel window) was extracted from the model's projected soil erosion map. The comparison between the modeled soil loss from InVEST and the estimated soil loss from observed sites were assessed by computing coefficient of determination (R^2) and root mean square error (RMSE) to affirm the precision of the findings.

Conversion Models used for estimating net soil erosion from ^{137}Cs activity

- **Simplified Mass Balance Model / Mass Balance Model I**: Zhang *et al.* (1990) introduced a simplified mass balance model, which assumes that all ^{137}Cs fallout occurred in 1963, rather than over a longer period from the mid-1950s to the mid-1970s. Mass balance models consider both the inputs and losses of ^{137}Cs to and from the soil profile since the onset of ^{137}Cs fallout. For an eroding site (A(t)<Aref), assuming a constant erosion rate R (m m-2 yr-1), the total 137Cs inventory (A , Bq m-2) for year t (yr) can be expressed as:

$$A(t) = A_{ref}(1 - P\left(\frac{R}{d}\right))^{t-1963}$$

The above equation can be rearranged to derive the erosion rates as follows:

$$Y = \frac{10dB}{P}(1 - (1 - \frac{X}{100})^{\frac{1}{t-1963}})$$

where: Y = mean annual soil loss (t ha^{-1} yr^{-1}), d = depth of the plough or cultivation layer (m), B = bulk density of soil (kg m^{-3}), X = percentage reduction in total 137Cs inventory (defined as (A_{ref} -A)/A_{ref} * 100), A_{ref} = local ^{137}Cs reference inventory (Bq m^{-2}), A = measured total ^{137}Cs inventory at the sampling point (Bq m^{-2}), P = particle size correction factor for erosion.

- **Profile Distribution Model**: Soils, which are undisturbed like the ones found in forests, are believed to have depth distribution of ^{137}Cs. In such soils, the ^{137}Cs concentration decreases with depth which can be categorized by the equation given by Zhang *et al.,* 1990 and Walling & Quine, 1993:

$$A'(x) = A_{ref}\ (1 - e^{-x/h_0}\ )$$

where: A'(x) = amount of ^{137}Cs above the depth x (Bq m^{-2}), Aref = ^{137}Cs reference inventory (Bq m^{-2}), x = depth from soil surface (kg m^{-2}), h_0 = coefficient describing profile shape (kg m^{-2}).

If it is assumed that the complete ^{137}Cs deposition took place in 1963 and the vertical distribution (depth) of ^{137}Cs in the soil column remains constant over time, the rate of erosion Y at a specific location (where the total ^{137}Cs content Au (Bq m^{-2}) is lower than the reference inventory Aref (Bq m^{-2}) can be mathematically represented as:

$$Y = \frac{10}{(t-1963)P} ln(1 - \frac{X}{100})\ h_0$$

where: Y = annual soil loss (t ha^{-1} yr^{-1}), t = year of sample collection (yr), X = percentage ^{137}Cs loss in total inventory in respect to the local ^{137}Cs reference value (defined as (A_{ref} - A)/A_{ref} * 100), Au = measured total ^{137}Cs inventory at the sampling point (Bq m^{-2}).

3 | RESULTS AND DISCUSSION

Physiographic Analysis

The elevation and LULC characteristics of the area are depicted in *Fig. 4* and *Fig. 5*. Elevation within the area varied from 793 to 4785 m above mean sea level *Fig. 4 ,* ascending from the lesser Himalaya region in the southern part to the greater Himalayan region in the northern part. The slope analysis revealed that majority of the watershed falls under moderately steep sloping category (21.55%) and the slopes are prominently oriented towards the southern aspect (56.28%). The soils of watershed were predominantly sandy loam to loam in texture. TPI was also computed, which quantifies the elevation or position of a point in relation to the mean elevation of its neighboring areas. It gives an idea about the ruggedness of the terrain thus classifying it into the upper, middle and lower regions of a hillslopes in the landscape. Ridges or hilltops are indicated by the positive values of TPI whereas flat lands or valleys have negative TPI. In this study, the TPI values were classified into 5 classes, namely, valley, toe slope, back slope, shoulder slope and hilltop/ridge. Further analysis revealed that toe slope covered the majority of the area (24.95%) in the watershed. The watershed is dominantly covered by forests (63.40%) followed by scrublands (15.78%), agricultural lands (12.70%), permanent snow covered regions

(1.32%), settlement (0.32%) and waterbody (0.24%), as depicted in the LULC map (*Fig. 5*). Most of these parameters were combined for generating the physio-graphic or soil-landscape units map, for soil sampling as well as studying the influence on soil erosion. For this, the TPI map was combined with the aspect map, which resulted in the landform or hillslope-element map. After combining the slope orientation on landform, the LU/LC classes were combined with the hillslope element classes, which finally yielded 24 units of the physiography or soil-landscape units (*Fig. 6*). Toe Slope - Forest class accounting for 13.63% of the total area, covered majority of the watershed area. The areal distribution of different soil-landscape units are detailed in Table 1.

RUSLE Parameters

The average yearly R factor for the region estimated using IMD gridded data employing the rainfall-erosivity relationship given by Chen et al., 2023 ranged from 1524.46 to 1906.93 MJ mm ha^{-1} h^{-1} $year^{-1}$ (*Fig. 7*). The computed R factor values found to be slightly lesser compared to the values used by Kalambukattu *et al.* (2021) for soil erosion risk assessment of entire Uttarakhand state using geospatial modelling approach. Most prominent soil texture found in the region was sandy loam followed by loamy, silt loam and loamy sand soils. Soil analysis database containing sand, silt, clay, and organic matter content of collected soil samples was used to calculate the K factor which ranged from 0.030 to 0.050 t ha h ha^{-1} MJ^{-1} mm^{-1} in the study area. Among the different soil-landscape units, K-factor was found to be highest for Valley-Scrub lands, followed by Hilltop-Agricultural lands (Table 2). Among the different LULC types, the average K-factor was found to be highest in scrublands, followed by agricultural lands and forests. The K factor values in the study were found to be similar to the values reported by Kalambukattu *et al.,* 2017, in a watershed level study conducted in the nearby area. The K factor value spatially varied from 0.027 to 0.041 (*Fig. 8*).

LS factor in the area ranged from 0.03 to 21.41 (*Fig. 9*). Scrub lands were found to have the highest value of LS factor, followed by forest and agricultural lands. A similar range of LS factor values are also reported in previous studies conducted in Uttarakhand Himalayas (Kalambukattu *et al.,* 2021).

Different LULC classes were assigned different C and P factor values based on literature review, as indicated in the Table 3. The model required the C and P factor values to be incorporated in the form of a biophysical (.csv) table, and thus it was subsequently prepared.

Maximum Sediment Delivery Ratio (SDR_{max})

SDRmax is a theoretical value indicating the maximum sediment transported from a region, typically ranging from 0 to 1, with a default value of 0.8. This means 80% of eroded

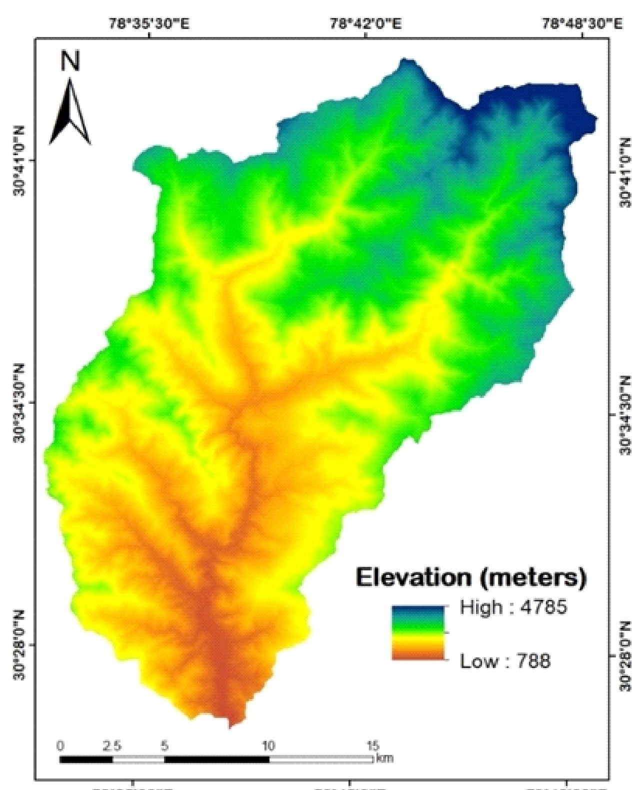

FIGURE 4 Elevation map of the study area

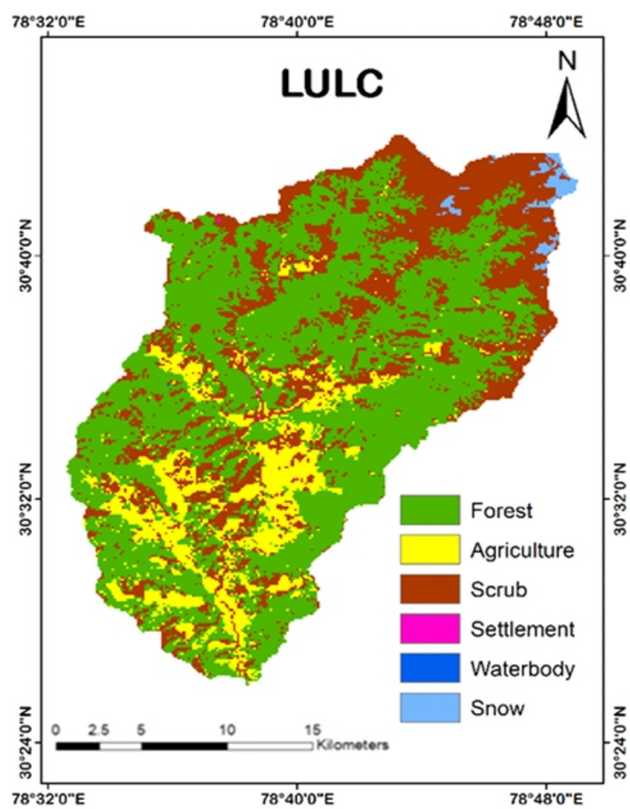

FIGURE 5 Land Use Land cover map of the watershed

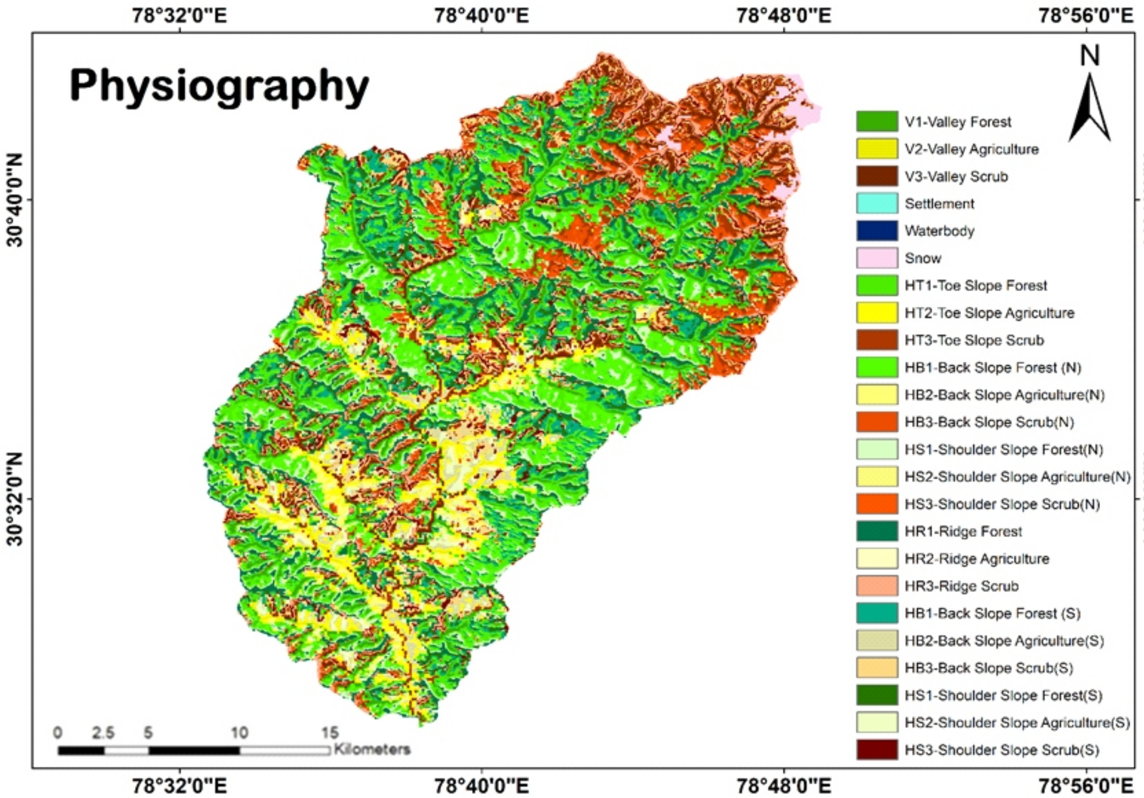

FIGURE 6 Physiographic unit map of the area

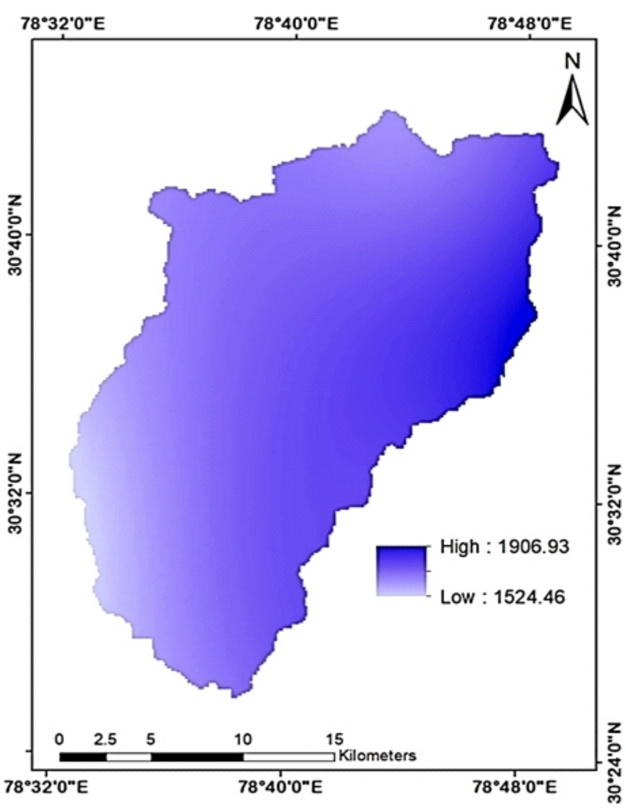

FIGURE 7 Spatial Distribution of R Factor

TABLE 1 Area Statistics of Physiographic Units

S.No.	Class	Area (ha)	Area (%)
1	V1-Valley Forest	2843	5.84
2	V2-Valley Agriculture	600.14	1.23
3	V3-Valley Scrub	1538.81	3.16
4	Settlement	30.23	0.062
5	Waterbody	5.23	0.010
6	Snow	483.95	0.995
7	HT1-Toe Slope Forest	6629.84	13.63
8	HT2-Toe Slope Agriculture	1966.33	4.04
9	HT3-Toe Slope Scrub	3417.36	7.03
10	HB1-Back Slope Forest (N)	4714.52	9.7
11	HB2-Back Slope Agriculture(N)	845.234	1.73
12	HB3-Back Slope Scrub(N)	1649.88	3.4
13	HS1-Shoulder Slope Forest(N)	3198.63	6.6
14	HS2-Shoulder Slope Agriculture(N)	435.25	0.895
15	HS3-Shoulder Slope Scrub(N)	1116.19	2.35
16	HR1-Ridge Forest	2507.16	5.15
17	HR2-Ridge Agriculture	241.016	0.495
18	HR3-Ridge Scrub	1889.48	3.88
19	HB1-Back Slope Forest (S)	4150.91	8.53
20	HB2-Back Slope Agriculture(S)	1370.72	2.81
21	HB3-Back Slope Scrub(S)	2712.48	5.57
22	HS1-Shoulder Slope Forest(S)	3156.86	6.5
23	HS2-Shoulder Slope Agriculture(S)	728.656	1.5
24	HS3-Shoulder Slope Scrub(S)	2296.94	4.72

TABLE 2 K-factor values for different Physiographic Units

Soil-Landscape Units	K-Factor
Valley-Forest	0.035
Valley-Agriculture	0.032
Valley-Scrub	0.045
Toe slope-Forest	0.043
Toe slope-Agriculture	0.034
Toe slope-Scrub	0.036
Back slope-Forest (N)	0.030
Back slope-Agriculture (N)	0.034
Back slope-Scrub (N)	0.032
Back slope-Forest (S)	0.032
Back slope-Agriculture (S)	0.034
Back slope-Scrub (S)	0.038
Shoulder-Forest (N)	0.032
Shoulder-Agriculture (N)	0.035
Shoulder-Scrub (N)	0.036
Shoulder-Forest (S)	0.032
Shoulder-Agriculture (S)	0.033
Shoulder-Scrub (S)	0.035
Ridge-Forest	0.030
Ridge-Agriculture	0.045
Ridge-Scrub	0.035

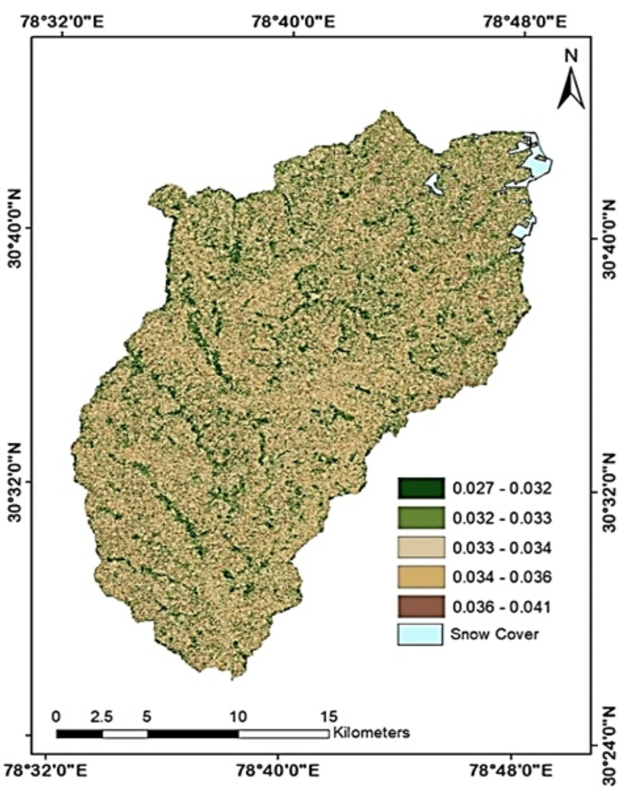

FIGURE 8 Spatial Distribution on K Factor

sediment is delivered to the stream, while 20% is deposited along the flow path. However, we have used an SDRmax of 0.6 reported from a watershed level study in Himalayan region (Singh *et al.,* 2019). Similar SDR value was also

TABLE 3 C and P Factors for the LULC Classes

Class	C-Factor	P-Factor
Forest	0.01	1
Agriculture	0.2	0.25
Scrub	0.1	1
Settlement	0.001	0.001
Waterbody	0	0
Snow	0	0

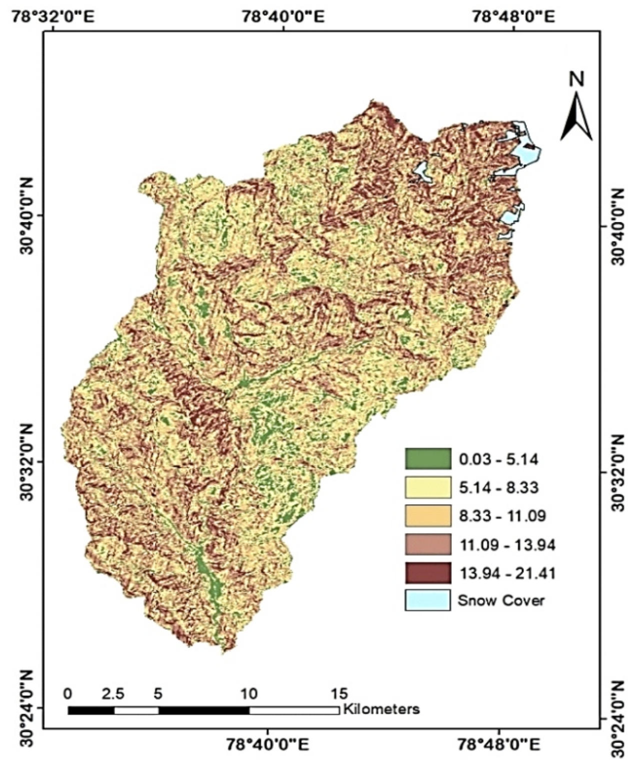

FIGURE 9 Spatial Distribution of LS Factor

reported in a study from Kandi region of Punjab (Yousuf *et al,* 2023). The model calculates potential SDR from each pixel using the connectivity index and a calibration parameter, ranging from 0 to 0.284. Higher SDR values mean that more sediment reaches the stream, while lower values mean less sediment does. Pixels near the streams have higher connectivity indices due to their proximity to stream pixels, while low connectivity areas are farther away. Thus, higher values cluster close to the stream, and lower values are dispersed further away.

Maximum Length of Slope (L_{max})

It is the longest flow path or maximum allowed length of slope from a pixel to it's nearest stream. As suggested and computed by Desmet and Govers, 1996, it can range from 122 to 333, but the default value which works for most of the terrains of similar kind is 122. Hence, the default value of 122 was taken for the L_{max} parameter in the present study.

Borselli k_b parameter

It is the measure of soil's ability to absorb water and is commonly used in agricultural watersheds to estimate runoff and storage. It functions as a calibration parameter that determines the shape of the relationship between hydrologic connectivity and the SDR. It ranges from 0.5 to 3.0 and the default value is normally taken as 2. In this study too, the default value of 2 was taken.

Borselli IC_0 parameter

It illustrates the hydrological linkage from the sources of sediment (landscape) to the sinks (streams). The value of IC_0 can be negative or positive depending upon the source or sink. It's default value given as 0.5 in the model's user guide (Sharp et al., 2018) was used in this study.

Threshold Flow Accumulation

The maximum number of upslope pixels that flow into a pixel before it is classified as a stream is termed the threshold flow accumulation. Generally, for hilly, mountainous regions, where the terrain ruggedness changes abruptly, 750 pixels are considered as the default value, which would be the minimum number of pixels to converge and form a stream. On the contrary, for flat lands or plains, where the terrain is less rugged, the value is taken between 1000-2000 pixels.

Watershed Boundary

The watershed boundary was delineated on ArcGIS 10.5 using the ALOS PALSAR DEM and the Hydrology toolbox. The watershed boundary, an important model input, was converted into ESRI Shapefile (.shp) format and further used in the model.

Model Outputs

Potential Average Annual Soil Loss

Annual soil loss in the region ranged from 0 to 24.384 tonnes ha^{-1} $year^{-1}$ (*Fig. 10*) or 0.381 t $pixel^{-1}$ yr^{-1}. The total soil erosion compared to Uttarakhand's estimated loss using the RUSLE model ranged from 0 to 250 t $ha^{-1}yr^{-1}$ (Kalambukattu *et al.,* 2021). The average annual erosion rate was 7.89 t ha^{-1} yr^{-1}, below Uttarakhand's soil loss tolerance limit as per Mandal and Sharda, 2011. Erosion from settlements, waterbodies, and snow-covered areas is negligible, thus not significantly affecting overall erosion. However, erosion from forests, agriculture, and scrublands is substantial, with average rates of 2.50, 10.83, and 16.86 t ha^{-1} yr^{-1}, respectively. The InVEST-SDR model applies to diverse regions, such as the, Huaihe region, China (Guo *et al.,* 2023), and Godavari Basin's watersheds (Kantharajan *et al.,* 2023) and the estimated erosion rates were comparable.

The sediment export capacity in the watershed ranged from 0 to 0.045 t $pixel^{-1}$ yr^{-1} (0 to 2.88 t ha^{-1} yr^{-1}), averaging 0.010 t $pixel^{-1}$ yr^{-1} (0.67 t ha^{-1} yr^{-1}). Sediment export values were estimated for three LU/LC types, excluding snow-covered areas, waterbodies, and settlements. Average sediment exports were 1.42 t ha^{-1} yr^{-1} for agriculture, 1.23 t ha^{-1} for scrub, and 0.15 t ha^{-1} for forests. Model data indicates agriculture has the highest sediment export, followed by scrublands and forests. Forest export is limited by litter and root-bound soil, while tillage in agricultural areas increases sediment export potential. Similar trends were found in Debie and Awoke, 2023.

The sediment retention capacity in the area ranged from 0 to 0.46 t $pixel^{-1}$ yr^{-1} (*Fig 10*), (0 to 29.44 t ha^{-1} yr^{-1}), with an average value of 0.272 t $pixel^{-1}$ yr^{-1} (17.45 t ha^{-1} yr^{-1}). This corresponds to the amount of sediment that could be maintained on a pixel, taking into account both on-pixel erosion and sediments from upslope pixels. With the exception of snow-covered areas, waterbodies, and settlement areas, sediment retention values were determined for three LU/LC categories. The average retained sediment found in agriculture, scrub lands, and forests was 21.96 t ha^{-1} yr^{-1}, 24.57 t ha^{-1}, and 13.43 t ha^{-1}, respectively. According to the modeled data, the agricultural fields with well-maintained terraces have the highest avoided export rates. The higher sediment retention values from the scrublands was estimated due to the persisting snow cover in the region for an extended duration of the year. The shrublands of the Konta watershed (Kantharajan *et al.,* 2023) also showed more sediment retention than the forest and cultivated lands.

Validation

Model predictions were validated using net soil loss values estimated from ^{137}Cs activity of soil samples collected from fifteen locations, including cultivated and uncultivated areas. A reference site within 5 km allowed meaningful comparisons with fields undergoing soil redistribution. Positive differences in erosion rates indicated deposition, while negative differences indicated erosion. Radionuclide activity was measured in Becquerel per square meter (Bq m-2), converting to soil erosion values in tons per hectare per year (t ha^{-1} yr^{-1}) utilizing various models from the methodology section. Soil loss values were extracted from modeled output rasters with different pixel windows to assess average soil loss for validating outputs (Table 4). The 7x7 pixel window yielded the best results comparing modeled gross erosion values and observed net erosion. Various pixel window sizes minimized errors from raster pixel edges, but some locations still risk class mixing due to nearby different land uses. Different window kernel sizes were considered to reduce land use conflicts, minimizing fluctuations in mean erosion values. The coefficient of determination (R^2), mean absolute error (MAE), and root mean square error (RMSE) assessed model accuracy (*Fig. 11*).

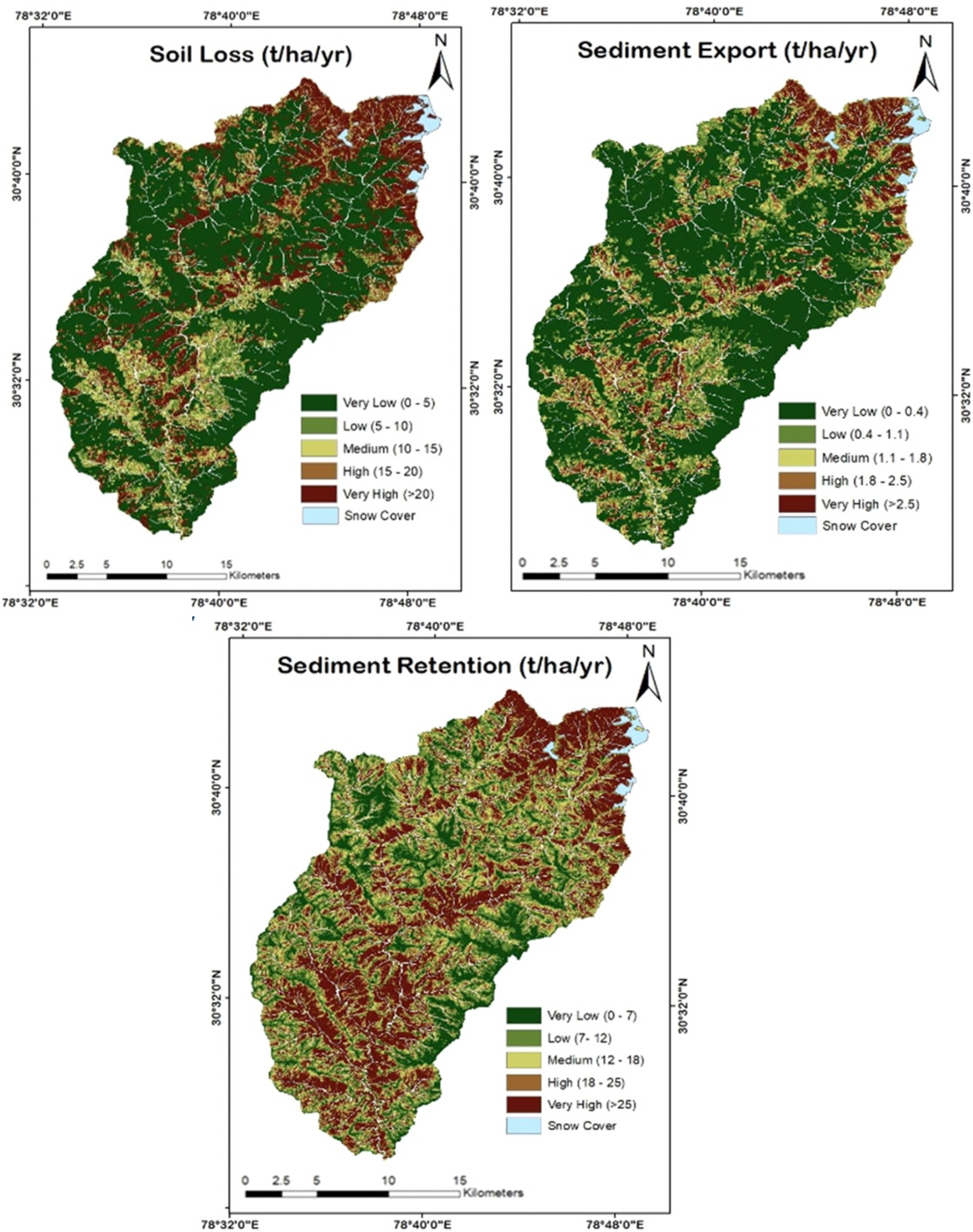

FIGURE 10 Spatial distribution maps of annual Soil Loss, Sediment Export and Sediment Retention

TABLE 4 Assessment of Observed versus Predicted Values

Points	Vegetation Type	Observed Net Soil Loss ($t\ ha^{-1}\ yr^{-1}$)	Predicted Gross Soil Loss ($t\ ha^{-1}\ yr^{-1}$)
1	Cultivated	4.8	2.4
2	Forest	2.9	6.9
3	Cultivated	14.5	23.3
4	Forest	4.0	9.8
5	Cultivated	10.0	9.4
6	Cultivated	1.6	9.5
7	Forest	3.7	14.2
8	Forest	4.7	12.6
9	Cultivated	0.0	0.8
10	Forest	8.0	8.4
11	Forest	2.1	1.6
12	Forest	0.0	1.8
13	Cultivated	1.3	2.4
14	Forest	6.4	5.7
15	Forest	7.3	6.6

The model evaluation indicators had suboptimal values. The ^{137}Cs approach measures net soil erosion, unlike the gross soil erosion measured by InVEST-SDR, which uses RUSLE to quantify all potential soil loss at a location. This discrepancy complicates comparing gross soil loss outputs to observed soil loss. The erosion rates from the model and radiotracer technique showed moderate agreement, as illustrated in *Fig. 11*. The evaluation yielded a coefficient of determination of 0.51, RMSE of 5.0, and MAE of 3.6. Both methods, despite varying magnitudes, captured similar patterns in erosion rates, as shown in *Fig 12*. If sediment redistribution were excluded, erosion rates would closely align with net soil erosion rates. Points 9 and 12 ($0.8\ t\ ha^{-1}\ yr^{-1}$ and $1.8\ t\ ha^{-1}\ yr^{-1}$) indicate deposition sites where observed net erosion is $0\ t\ ha^{-1}\ yr^{-1}$. Although validation results are not promising due to the study area's size, adding more 137Cs-based inventory points could enhance calibration and prediction of erosion rates. Gharibreza *et al.* (2021) compared soil loss from the ^{137}Cs method with RUSLE, showing their similarity, while Paolo Porto (2023) noted similar outputs for both models in the absence of deposition.

4 | CONCLUSIONS

The InVEST-SDR model predicted potential average annual soil loss ranging from 0 to $67.63\ t\ ha^{-1}\ yr^{-1}$. The majority (58.11%) of the region fell under the very low erosion class (0 - $20\ t\ ha^{-1}\ yr^{-1}$), with average soil erosion in forests, agriculture, and scrub lands at 5.26, 16.68, and $35.51\ t\ ha^{-1}\ yr^{-1}$, respectively. Scrub lands, covering 15.78% of the area, contributed significantly to soil loss, especially on ridges with sparse vegetation. Sediment export calculations ranged from 0 to $10.5\ t\ ha^{-1}\ yr^{-1}$, with 59.45% of the region in the very low sediment export class (0-$0.4\ t\ ha^{-1}yr^{-1}$). Average sediment export for forests, agriculture, and scrub

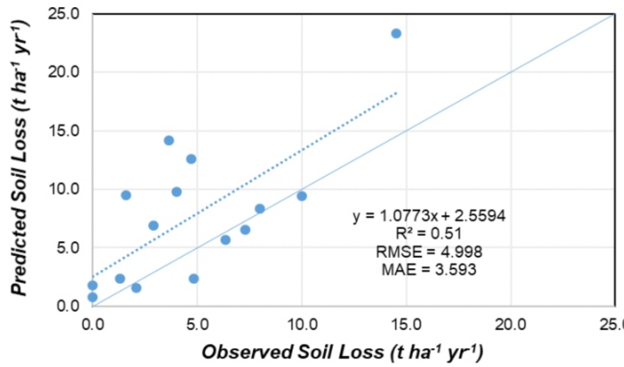

FIGURE 11 Scatter graph of Observed and Predicted Soil Erosion

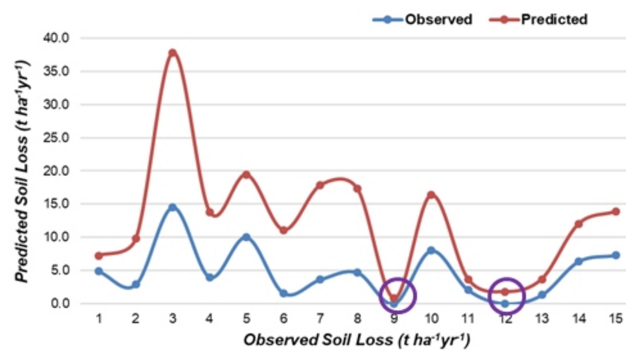

FIGURE 12 Pattern Map of Observed Net Soil Loss versus Predicted Gross Soil Loss

lands was 0.37, 2.29, and $3.52\ t\ ha^{-1}\ yr^{-1}$, respectively. Agricultural lands showed high sediment export due to poor management practices and proximity to water sources. Sediment retention, ranging from 0 to $60\ t\ ha^{-1}\ yr^{-1}$, was higher in areas near streams, with agricultural lands retaining $25.84\ t\ ha^{-1}\ yr^{-1}$ on average. Forests retained $20.73\ t\ ha^{-1}\ yr^{-1}$ and scrub lands $25.44\ t\ ha^{-1}\ yr^{-1}$. Higher retention in the scrubland was seen mainly at the top portion of the region, which experiences prolonged snow cover for a significant portion of the year. For a data scarce region and a highly rugged terrain, the model works well explaining 51% of the variance in observed soil loss, indicating potential for improvement with more validation points or net soil erosion values from the model. However, the model's sensitivity to the Kb values can affect its output hence, calibration of the model needs to be done with measured sediment data before using it for any land management practices. Cover management and support practices factor also significantly influenced the model results, highlighting the impact of poor agricultural practices on erosion and sediment dynamics, although these can be improved by using a higher resolution DEM or detailed LU/LC classification. The results from the model can be utilized for identifying the erosion hotspots and prioritizing the sub-watersheds for different soil and water conservation practices. This model can provide an end to end interface for traders starting from analyzing and estimating the ecosystem service, monetizing it and providing both qualitative and quantitative assessment for any structures made (dams, bridges) or structures installed (solar parks, transmission towers) in these rugged terrains.

ACKNOWLEDGMENTS

The authors sincerely thank the Indian Space Research Organization (ISRO) for providing financial support under Earth Observation Applications Mission (EOAM) Project (ISRO/DOS) on Mountain Ecosystem Processes and Services - Phase - II -'Soil Erosion Estimation based on Radio Tracer Technique and Soil Quality Assessment in Mountainous Landscape of North-West Himalaya', which made this research possible. We express our gratitude to the Director, Indian Institute of Remote Sensing (IIRS) for providing all the necessary facilities and support for this research.

CONFLICT OF INTEREST

The authors declare that they have no known competing financial interests or personal relationships that could have appeared to influence the work reported in this paper.

DATA AVAILABILITY STATEMENT

The geospatial and climate datasets used in the study could be obtained from the respective sources cited in the text. The soil and FRN ^{137}Cs databases generated and used during the research work are currently not publicly available, as indian institute of remote sensing (IIRS), indian space research organization (ISRO), department of space, government of india sponsored the project.

AUTHOR'S CONTRIBUTION

Conceptualization: AS, JGK and SK; Methodology: AS, JGK and SK; Formal analysis, Data collection, analysis and investigation: AS and JGK; Writing original draft preparation: AS and JGK; Visualization - AS, Writing-review and editing AS and JGK; Supervision: JGK and SK. All authors read and approved the final manuscript.

REFERENCES

Abhisek Kumar Singh, S. Kumar, S. Naithani, J. George K (2019). Soil erosion and sediment yield estimation using remote sensing data and GIS of watershed in North West Himalayan region. Indian Journal of Soil Conservation, 47(3): 143-147.

Achu, A. L., & Thomas, J. (2023). Soil erosion and sediment yield modeling in a tropical mountain watershed of the southern Western Ghats, India using RUSLE and Geospatial tools. Total Environment Research Themes, 8, 100072. https://doi.org/10.1016/j.totert.2023.100072.

Boardman, J. (2021). How much is soil erosion costing us? Geography, 106(1), 32–38.

Borselli, L., Cassi, P., & Torri, D. (2008). Prolegomena to sediment and flow connectivity in the landscape: A GIS and field numerical assessment. Catena, 75(3), 268–277.

Bouguerra, S., & Jebari, S. (2017). Identification and prioritization of sub-watersheds for land and water management using InVEST SDR model: Rmelriver basin, Tunisia. Arabian Journal of Geosciences, 10(15), 1–9. https://doi.org/10.1007/s12517-017-3104-z.

Chen, W., Huang, Y. C., Lebar, K., & Bezak, N. (2023). A systematic review of the incorrect use of an empirical equation for the estimation of the rainfall erosivity around the globe. Earth-Science Reviews, 238(July 2022), 104339. https://doi.org/10.1016/j.earscirev.2023.10 4339.

Debie, E., & Awoke, Z. (2023). Assessment of the effects of land use/cover changes on soil loss and sediment export in the Tul Watershed, Northwest Ethiopia using the RUSLE and InVEST models. International Journal of River Basin Management, 1-16.

Degife, A., Worku, H., & Gizaw, S. (2021). Environmental implications of soil erosion and sediment yield in Lake Hawassa watershed, south-central Ethiopia. Environmental Systems Research, 10(1). https://doi.org/10.1186/s40068-021-00232-6.

Desmet, P. J. J., & Govers, G. (1996). A GIS procedure for automatically calculating the USLE LS factor on topographically complex landscape units. Journal of Soil and Water Conservation, 51(5), 427-433.

Durigon, V. L., Carvalho, D. F., Antunes, M. A. H., Oliveira, P. T. S., & Fernandes, M. M. (2014). NDVI time series for monitoring RUSLE cover management factor in a tropical watershed. International Journal of Remote Sensing, 35(2), 441–453.

Gharibreza, M., Bahrami Samani, A., Arabkhedri, M., Zaman, M., Porto, P., Kamali, K., & Sobh-Zahedi, S. (2021). Investigation of on-site implications of tea plantations on soil erosion in Iran using 137 Cs method and RUSLE. Environmental Earth Sciences, 80, 1-14.

Guo, Z., Yan, Z., PaErHaTi, M. E. Z. T., He, R., Yang, H., Wang, R., & Ci, H. (2023). Assessment of soil erosion and its driving factors in the Huaihe region using the InVEST-SDR model. Geocarto International, 38(1). https://doi.org/10.1080/10106049.2023.2213208.

Kalambukattu, J., & Kumar, S. (2017). Modelling soil erosion risk in a mountainous watershed of Mid-Himalaya by integrating RUSLE model with GIS. EURASIAN JOURNAL OF SOIL SCIENCE (EJSS), 6(2), 92–92. https://doi.org/10.18393/ejss.286442.

Kalambukattu, J.G., Kumar, S., & Hole, R. M. (2021). Geospatial modelling of soil erosion and risk assessment in Indian Himalayan region - A study of Uttarakhand state. Environmental Advances, 4 (February), 100039. https://doi.org/10.1016/j.envadv.2021.100039.

Kantharajan, G., Govindakrishnan, P. M., Singh, R. K., Natalia, E. C., Jones, S. K., Singh, A. & Lal, K. K. (2023). Quantitative assessment of sediment delivery and retention in four watersheds in the Godavari River Basin, India, using InVEST model - an aquatic ecosystem services perspective. Environmental Science and Pollution Research, 30(11), 30371-30384.

Kumar, S., David Raj, A., Mariappan, S. et al. Application of fallout radionuclide - ^{137}Cs for estimating soil erosion in steep hillslopes with diverse land use of North-western Indian Himalayas. Discov Environ 2, 105 (2024). https://doi.org/10.1007/s44274-024-00131-4.

Karydas, C., Panagos, P. and Gitas, I. Z. (2014): A classification of water erosion models according to their geospatial characteristics, Int. J. Digit. Earth, 7, 229-250, doi.org/10.1080/17538947.2012.67 1380.

Mandal, D., & Sharda, V. N. (2011). Assessment of permissible soil loss in India employing a quantitative bio-physical model. CURRENT SCIENCE, 100(3).

Pai D.S., Latha Sridhar, Rajeevan M., Sreejith O.P., Satbhai N.S. and Mukhopadhyay B., 2014: Development of a new high spatial resolution (0.25° × 0.25°) Long period (1901-2010) daily gridded rainfall data set over India and its comparison with existing data sets over the region; MAUSAM, 65, 1(January 2014), pp1-18.

Porto, P. (2023). Combining plot observations and 137Cs measurements to provide estimates of soil erosion rate during the last six decades: results from a cultivated area in Southern Italy. Journal of Soils and Sediments, 23(12), 4223-4234.

Ramachandran, S., Jena, R.K., Ray, P., Padua, Shelton., Borah, A.J., Ray, S.K. 2023. Soil erosion assessment in the hilly terrain of Arunachal Pradesh, India through integrated approach of RUSLE and geospatial technology. *Indian J. Soil Cons.,* 51(3) 171-180 DOI: 10.59797/ijsc.v51.i3.133

Rogowski, A.S. and Tamura, T. 1965. Movement of ^{137}Cs by Runoff, Erosion and Infiltration on the Alluvial Captina Silt Loam. *Health Physics,* 11(12):1333-1340. https://doi.org/10.1097/00004032-196512000-00010.

Sharp, R., Chaplin-Kramer, R., Wood, S., Guerry, A., Tallis, H., Ricketts, T., Nelson, E., Ennaanay, D., Wolny, S., Olwero, N., Vigerstol, K., Pennington, D., Mendoza, G., Aukema, J., Foster, J., Forrest, J., Cameron, D. R., Arkema, K., Lonsdorf, E., & Douglass, J. (2018). InVEST User's Guide. https://doi.org/10.13140/RG.2.2.32693.78567.

Sharpley A N, W. J. R. (1993). EPIC-Erosion/Productivity Impact Calculator: 1. Model Documentation. Technical Bulletin No. 1768.

Swarnkar S, Malini A, Tripathi S, Sinha R (2018) Assessment of uncertainties in soil erosion and sediment yield estimates at ungauged basins: an application to the Garra River basin India. Hydrol Earth Syst Sci 22(4):2471–2485.

Viney, N. R., & Sivapalan, M. (1999). A conceptual model of sediment transport: application to the Avon River Basin in Western Australia. Hydrological Processes, 13(5), 727–743.

Walling, D. E., and Quine, T. A. 1993. Use of caesium-137 as a tracer of erosion and sedimentation: Handbook for the application of the caesium-137 technique. UK Overseas Development Administration Research Scheme R4579.

Wang, X., Liu, X., Long, Y., Liang, W., Zhou, J., & Zhang, Y. (2020). Analysis of Soil retention service function in the North Area of Guangdong based on the InVEST model. IOP Conference Series: Earth and Environmental Science, 510(3). https://doi.org/10.1088/1755-1315/510/3/032011.

Williams, J. R. (1978). A sediment graph model based on an instantaneous unit sediment graph. Water Resources Research, 14(4), 659–664.

Yousuf, Abrar., Sharma, Navneet., Benipal, Kaur, Amanpreet., Singh, M.J., Bhat, Amin, Mohammad., and Dahiphale, Pravin., 2023. Integrating RUSLE and SDR in GIS framework for assessment of soil erosion and sediment yield in Kandi region of Punjab. *Indian J. Soil Cons.,* 51(3) 188-195 DOI: 10.59797/ijsc.v51.i3.135.

Zhang, X. B., Higgitt, D. L. and Walling, D. E. (1990): A preliminary assessment of the potential for using caesium-137 to estimate rates of soil erosion in the Loess Plateau of China. Hydrol. Sci. J. 35: 267-276.

How to cite this article: Akanksha Singh, Justin George Kalambukattu, Suresh Kumar. 2025. Assessing Soil Erosion and Sediment Dynamics in the Balganga Watershed, Uttarakhand: Integration of InVEST-SDR and Fallout Radionuclide (FRN) ^{137}Cs Method. *Indian J. Soil Cons.,* 53(1): 1-16.